International Journal on Recent and Innovation Trends in Computing and Communication
ISSN: 2321-8169 Volume: 10 Issue: 1s
DOI: https://doi.org/10.17762/ijritcc.v10i1s.5821
***Article Received**: 26 August 2022 **Revised**: 31 October 2022 **Accepted**: 23 November 2022*

HBMFTEFR: Design of a Hybrid Bioinspired Model for Fault-Tolerant Energy Harvesting Networks via Fuzzy Rule Checks

Jaya Dipti Lal[a,*], Dr Dolly Thankachan[b]
[a]*Assistant Professor, Electronics & Tc Department, S.G.S.I.T.S. Indore (MP), PhD Scholar, Oriental University Indore (M.P.), jayadiptilal@yahoo.co.in, (M)8878715021*
[b]*Associate Professor and Head, Department of Electrical and Electronics Engineering Oriental University Indore (M.P.), drdolly@orientaluniversity.in,(M)9479273510*
*Corresponding author Tel.: +91-8878715021; *E-mail: jayadiptilal@yahoo.co.in

ABSTRACT
Designing energy harvesting networks requires modelling of energy distribution under different real-time network conditions. These networks showcase better energy efficiency, but are affected by internal & external faults, which increase energy consumption of affected nodes. Due to this probability of node failure, and network failure increases, which reduces QoS (Quality of Service) for the network deployment. To overcome this issue, various fault tolerance & mitigation models are proposed by researchers, but these models require large training datasets & real-time samples for efficient operation. This increases computational complexity, storage cost & end-to-end processing delay of the network, which reduces its QoS performance under real-time use cases. To mitigate these issues, this text proposes design of a hybrid bioinspired model for fault-tolerant energy harvesting networks via fuzzy rule checks. The proposed model initially uses a Genetic Algorithm (GA) to cluster nodes depending upon their residual energy & distance metrics. Clustered nodes are processed via Particle Swarm Optimization (PSO) that assists in deploying a fault-tolerant & energy-harvesting process. The PSO model is further augmented via use of a hybrid Ant Colony Optimization (ACO) Model with Teacher Learner Based Optimization (TLBO), which assists in value-based fault prediction & mitigation operations. All bioinspired models are trained-once during initial network deployment, and then evaluated subsequently for each communication request. After a pre-set number of communications are done, the model re-evaluates average QoS performance, and incrementally reconfigures selected solutions. Due to this incremental tuning, the model is observed to consume lower energy, and showcases lower complexity when compared with other state-of-the-art models. Upon evaluation it was observed that the proposed model showcases 15.4% lower energy consumption, 8.5% faster communication response, 9.2% better throughput, and 1.5% better packet delivery ratio (PDR), when compared with recently proposed energy harvesting models. The proposed model also showcased better fault prediction & mitigation performance when compared with its counterparts, thereby making it useful for a wide variety of real-time network deployments.

Keywords: Energy, Harvesting, Fault, Tolerance, Bioinspired, Communication, GA, PSO, ACO, TLBO, Fuzzy

1. Introduction

Energy harvesting model design for wireless networks is a multidomain task, that involves analysis of nodes, evaluation of faults, estimation of mitigation strategies, transfer of energy between nodes, QoS maintenance via Machine Learning Models, etc. To implement a high-efficiency energy harvesting model, researchers & network designers are required to analyze different network & node-specific parameters. For instance, a typical fault-tolerance aware energy harvesting model that uses Cuckoo Search Optimization (CSO) is depicted in figure 1, wherein deep reinforcement learning (DRL) is used for deployment of continuous training & energy optimization processes. The model initially uses an energy harvesting block which allows large scale wireless sensor networks (WSNs) to share energy between different nodes. This energy sharing process is accompanied with a pre-processing block, that assists in reducing probability of faults via estimation of low energy nodes, evaluation of high-trust nodes, and identification of nearby nodes for better communication performance.

International Journal on Recent and Innovation Trends in Computing and Communication
ISSN: 2321-8169 Volume: 10 Issue: 1s
DOI: https://doi.org/10.17762/ijritcc.v10i1s.5821
***Article Received**: 26 August 2022 **Revised**: 31 October 2022 **Accepted**: 23 November 2022*

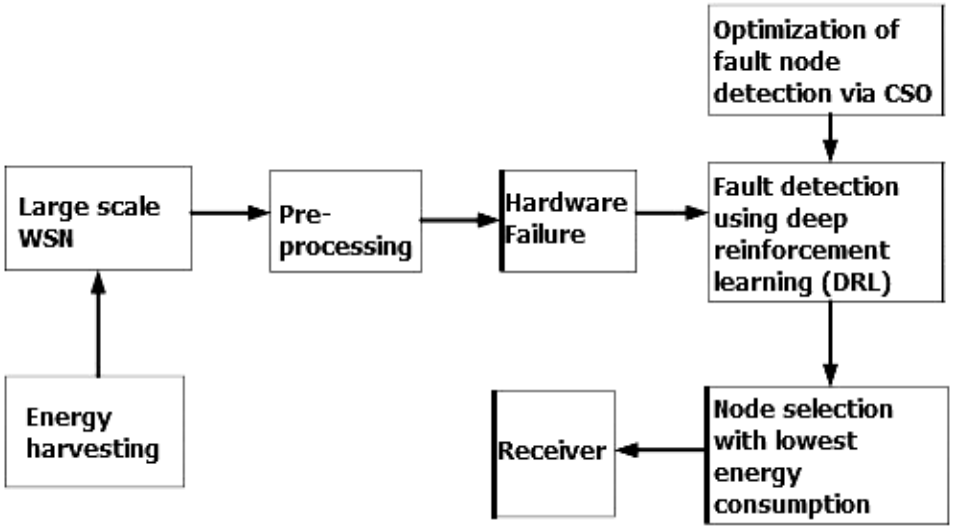

Figure 1. Design of a typical energy harvesting model for fault tolerant wireless sensor networks

The identified nodes are evaluated for hardware failure, via a deep reinforcement learning (DRL) model, that assists in identification of faulty nodes, and removing them from the communication process. Selected nodes are filtered via a fitness evaluation function described by equation 1, which assists in identification of nodes with higher energy and lower distance metrics,

$$f_i = \left(\frac{\sqrt{(x_1 - x_2)^2 + (y_1 - y_2)^2}}{E_{final} - E_{initial}} \right)_i \quad \dots (1)$$

Where, (x, y) represents location of the nodes, while E_{final}, & $E_{initial}$ represents final & initial energy of the nodes involved in the communication process. Similar models are proposed by researchers, which assist in optimizing energy consumption via identification of high-trust nodes via different fitness functions. A review of such energy efficient & fault tolerant models, along with their nuances, advantages, limitations, and future research scopes is discussed in the next section of this text. Based on this discussion it was observed that some of these models are affected by internal & external faults, which increase energy consumption of affected nodes. While, deployment of other fault tolerant models is highly complex, and increases computational complexity, storage cost & end-to-end processing delay of the network, which reduces its QoS performance under real-time use cases. To overcome these issues, section 3 discusses design of a hybrid bioinspired model for fault-tolerant energy harvesting networks via fuzzy rule checks. The proposed model was evaluated in section 4, and compared in terms of different performance metrics with various state-of-the-art models. Finally, this text concludes with some interesting observations about the proposed model, and recommends methods to further improve its performance.

2. Literature Review

A wide variety of energy harvesting and fault tolerant models are proposed by researchers, and each of them have different computational characteristics, which determine their deployment capabilities. For instance, work in [1, 2, 3] proposes Radio Frequency (RF) based energy harvesting for IoT devices, data and energy integrated network (DEIN), and improved uneven clustering protocol (IUCP) for reducing node-level energy consumption during network communications. Similar models are discussed in [4, 5, 6], which discuss deployment of Device-Selective Energy Requests, Upper Confidence Bound (UCB), and time-synchronized channel hopping (TSCH) with energy savvy network joining strategies. These models showcase high energy efficiency due to intrinsic use of energy preservation techniques, which assists in reducing continuous power use under different communication scenarios. But these models are highly complex, which limits their usability & scalability performance. To overcome this limitation, work in [7] proposes use of Energy-Efficient Task Offloading via Differential Evolution, and Edge Computing Model, which assists in low power, and high efficiency network deployments. This model uses cloud computing to perform highly complex tasks, and offloads low power tasks to lower performance nodes. Due to which, the model showcases better energy efficiency, with higher throughput capabilities. Inspired by this model, work in [8, 9, 10] proposes Energy Harvesting Intelligent Relay Selection Protocol (EH-IRSP),

International Journal on Recent and Innovation Trends in Computing and Communication
ISSN: 2321-8169 Volume: 10 Issue: 1s
DOI: https://doi.org/10.17762/ijritcc.v10i1s.5821
***Article Received**: 26 August 2022 **Revised**: 31 October 2022 **Accepted**: 23 November 2022*

Online Energy Scheduling, and dynamic programming (DP) that assists in improving throughput while maintaining high energy efficiency under different network scenarios.

Models that utilize joint caching and user association for energy efficient operations [11], fast time fair energy allocation model (FTF) [12], Capacitor Charging Management Schemes [13], and Extended Hierarchical Clustering (EHC) [14] are also discussed by researchers, which aim at reducing power consumption via redundancy estimation and removal from wireless sensor networks. Similar models are discussed in [15, 16, 17], wherein researchers have proposed use of Threshold-Oriented and Energy-Harvesting Enabled Multilevel Stable Election Protocol (TEMSEP), and Distributed Deep Reinforcement Learning (DDRL) for Energy Harvesting Virtualized Small Cells. These models are capable of incorporating energy levels with distance and other measures in order to improve energy efficiency of WSN deployments. Extensions to these models are discussed in [19, 20, 21], wherein Optimal Resource Allocation, Orientation-Independent Multiple Input Energy Efficient Networks, Multiple Featured Actor & Critic based Relay Selection Model are discussed for dynamic networks. These models showcase utilization of both network & node related parameters to incorporate energy efficiency in wireless scenarios.

Fault tolerant methods are also required to improve efficiency of wireless networks under real-time scenarios. Work in [22, 23, 24] proposes Maximum Likelihood Event Localization (MLEM), fault-tolerance using repairing points in clusters, and Fault-Tolerant Clustering Topology (FTCT) for improving efficiency during different network faults. These models are further extended via use of node-link failure fault tolerance model (NLFFT) with improved quadratic minimum spanning tree [25], static backup and dynamic timing monitoring (SBDTM) [26], Kuatz Fault Tolerance [27], and Adaptive Fault Tolerance (AFT) [28] models that assists in reducing network faults via augmentation of different network parameters. Extensions to these models are discussed in [29, 30, 31], which discuss use of Dual Cluster Heads Cooperation (CoDuch), Delay Aware Regional Fault-Tolerant Routing Model, and distributed node classification for improved fault tolerance performance under real-time conditions. These models showcase slower performance due to use of highly complex computational models. This performance can be improved via discrete particle swarm optimization (DPSO) based oft real-time fault-tolerant task allocation algorithm (FTAOA) [32], collaborative sensor fault detection (CSFD) [33], and Energy-Efficient and Cooperative Fault- Tolerant Communications [34], which assist in estimating network-level faults via pattern analysis. But none of these models combine fault tolerance with energy harvesting, which limits their practical usability. To improve this usability, next section proposes design of a novel Hybrid Bioinspired Model for Fault-Tolerant Energy Harvesting Networks via Fuzzy Rule Checks. The proposed model was tested under different network conditions, and performance was compared w.r.t. various reviewed models for real-time analysis.

3. Design of the proposed Hybrid Bioinspired Model for Fault-Tolerant Energy Harvesting Networks via Fuzzy Rule Checks

From the literature review it can be observed that a wide variety of energy harvesting models with fault tolerance have been proposed by researchers. Each of these models have devised customized Machine Learning solutions for improving their security & QoS performance metrics. But these models require continuous training, which increases their computational complexity, storage cost & end-to-end processing delay, and reduces QoS performance under real-time use cases.

To overcome these limitations, a novel light weight model that uses Genetic Algorithm (GA) for distance & energy-aware node clustering, Particle Swarm Optimization (PSO) for achieving fault-tolerance & energy-harvesting, and hybrid Ant Colony Optimization (ACO) Model with Teacher Learner Based Optimization (TLBO), which assists in value-based fault prediction & mitigation operations is discussed in this text. Overall flow of the proposed model is depicted in figure 2, wherein different bioinspired models along with their process flows can be observed.

International Journal on Recent and Innovation Trends in Computing and Communication
ISSN: 2321-8169 Volume: 10 Issue: 1s
DOI: https://doi.org/10.17762/ijritcc.v10i1s.5821
***Article Received**: 26 August 2022 **Revised**: 31 October 2022 **Accepted**: 23 November 2022*

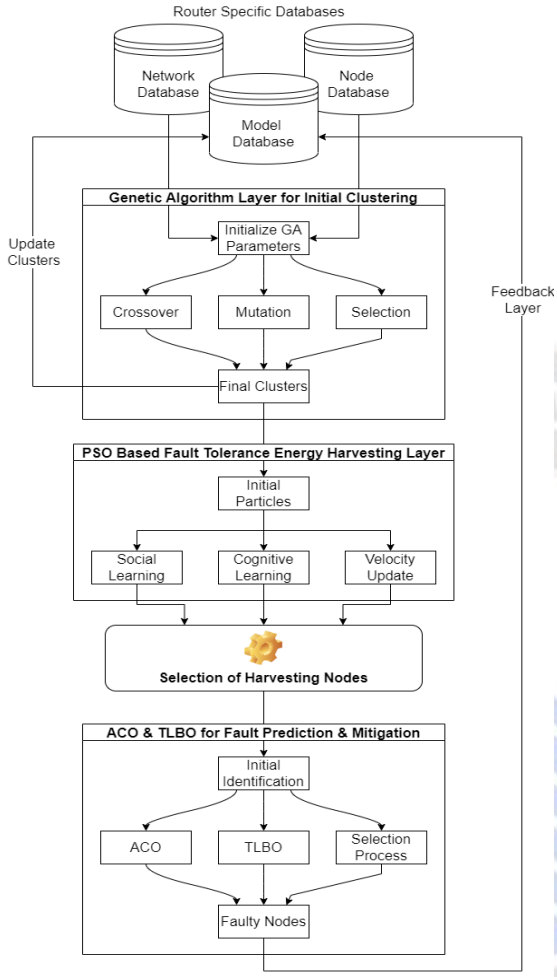

Figure 2. Overall flow for the proposed GA, PSO, ACO & TLBO Model for QoS-aware fault tolerance

From the figure it can be observed that initial clustering is performed by GA, which assists in delay & energy-aware grouping of nodes. These nodes are further processed via PSO-based fault tolerance model, that assists in identification of energy-harvesting node sets. These node sets are given to ACO & TLBO Model for value-based fault checking, that assists in continuous QoS improvement under different communication scenarios. Design of the proposed model is divided into different sub modules, and design for each of these modules is discussed in separate sub-sections of this text. This will assist readers to implement these models in part(s) or as a whole, depending upon their network requirements.

3.1. Design of the GA Layer for initial clustering

In the network, various databases are stored on router nodes, which includes network, node, and model databases. Each of these database stores an entity specific set of information, that assists in identification of different parameters. For instance, Network Database stores information about current bandwidth, data rate, Received Signal Strength Indicator (RSSI), capacity, temporal node performance, link quality, etc. which are related to network deployment. While, node-level information including approximate locations, energy levels, energy models, capacity of nodes, etc. is stored on the node database. The model database stores decision information, which includes routing rules, energy threshold levels, etc. All this information is provided to the GA Model, which assists in estimation of initial clusters. This clustering is performed via the following process,

- Initialize GA Parameters,
  - Number of iterations (N_i)
  - Number of solutions (N_s)
  - Learning rate (L_r)
  - Maximum number of clusters ($C(Max)$)
- Initially mark each solution as 'to be modified'
- For each iteration between 1 to N_i
  - For each solution between 1 to N_s
    - If the solution is marked as 'not to be modified', then go to the next solution.
    - Else, Generate a solution via the following process,
- Initialize number of clusters (N_c) stochastically via equation 2,

$$N_c = STOCH\big(2, C(Max)\big) \dots (2)$$

Where, $STOCH$ represents a stochastic Markovian process for generating stochastic numbers for different sets.

- Based on this, divide the nodes stochastically into N_c clusters via k Means, via evaluation of distance, energy and node capacity-based comparison metric which is evaluated via equation 3,

$$d_k = \frac{E(Node) * C(Node)}{\sqrt{\big(x(Node) - x(Centroid)\big)^2 + \big(y(Node) - y(Centroid)\big)^2}} \dots (3)$$

Where, d_k represents distance metric for k Means, while $E(Node)$ & $C(Node)$ represents residual energy & capacity of the node, and (x, y) represents current location of the nodes respectively.

- Based on this distance metric, nodes are clustered into N_c clusters, and a fitness function is evaluated via equation 4,

$$f_i = \frac{\sum_{i=1}^{N_c} \sum_{j=1}^{N(n)_i} \frac{d_{k_i} - d_{k_j}}{N(n)_i}}{N_c} \dots (4)$$

Where, $N(n)_i$ represents number of nodes present in the i^{th} cluster.

- This fitness value is evaluated for each solution, and a fitness threshold is calculated via equation 5 as follows,

International Journal on Recent and Innovation Trends in Computing and Communication
ISSN: 2321-8169 Volume: 10 Issue: 1s
DOI: https://doi.org/10.17762/ijritcc.v10i1s.5821
***Article Received**: 26 August 2022 **Revised**: 31 October 2022 **Accepted**: 23 November 2022*

$$f_{th} = \sum_{i=1}^{N_s} f_i * \frac{L_r}{N_s} \dots (5)$$

- Solutions with fitness $f_i > f_{th}$ are marked as 'to be modified', while other solutions are marked as 'not to be modified'

- This process is repeated for N_i iterations, and solution with minimum fitness value is selected, and its clustering configuration is used for final clustering of nodes.

Based on this process, nodes are initially clustered into a set of N_c clusters, and each cluster is processed via a PSO Model for fault-tolerant energy harvesting with tolerance to improve routing effectiveness. This process is discussed in the next section of this text.

3.2. Designing the PSO layer for fault tolerant energy harvesting

After nodes are clustered with similar energy, better capacity, and lower distance from centroid, which assists in identification of clusters that might have faults during future communications. To perform this task, a PSO based model is used, which assists in segregating node clusters, based on their temporal performance. This model works via the following process,

- Initialize PSO parameters,
  - Number of particles (N_p)
  - Number of iterations (N_i)
  - Cognitive learning rate (L_c)
  - Social learning rate (L_s)
- Determine energy model for each node, and evaluate the following parameters,
  - Energy needed for transmission ($E(T)$)
  - Energy needed for reception ($E(R)$)
  - Energy needed during idle mode ($E(I)$)
  - Energy needed for waking up from sleep mode ($E(W)$)
  - Time needed for waking up from sleep mode ($T(W)$)
- Based on this model, generate initial particles via the following process,
  - For each cluster, evaluate cluster fitness via equation 6 as follows,

$$C_f = \sum_{i=1}^{N(n)} \frac{d_{k_i} - d_k(head)}{N(n)} * \left[\frac{T(W) * E(Max)}{\left(\begin{matrix} E(T) + E(R) + \\ E(I) + E(W) \end{matrix} \right) * Max(T(W))} \right] \dots (6)$$

Where, $E(Max)$ & $Max(T(W))$ represents maximum energy level of node, and maximum wake up time between different node configurations.

  - For each particle in 1 to N_p, perform the following tasks,
    - Stochastically shift nodes with higher d_k values to clusters with lower C_f values.
    - Evaluate particle velocities based on these shifts via equation 7,

$$PV(i) = \sum_{j=1}^{N_c} C_f(j) * \frac{L_r}{N_c} \dots (7)$$

    - Initially mark, $PBest = PV$
    - Mark the particle with highest PV as $GBest$ via equation 8,

$$GBest = Max\left[\bigcup_{i=1}^{N_p} PV(i) \right] \dots (8)$$

- For each iteration in 1 to N_i, perform the following tasks,
  - Update particle fitness via equation 9,

$$PV(New) = r * PV(Old) + L_c * [PV(Old) - PBest] + L_s[PV(Old) - GBest] \dots (9)$$

Where, r represents a stochastic number between the range $r \in (0.1, 1)$

  - Based on this value of PV, shift nodes between clusters to obtain required particle velocities.
  - Update $PBest$, if $PBest > PV(New)$
  - Similarly, update $GBest$ via equation 8 to obtain new particle sets
- At the end of the final iteration, identify particle with highest velocity, and use its configuration for the energy harvesting process.

After selection of final cluster configurations, nodes in clusters with lowest d_k values are marked as 'faulty' nodes, and are not used during communication sequences. Instead, these nodes are used as backup energy nodes, and are used for energy harvesting by nodes with higher d_k values. Due to this process, number of nodes needed during route selection are minimized, which reduces communication delays. The 'non faulty' clusters are further processed via the hybrid ACO & TLBO Model for identification & mitigation of faults. Design of this model is discussed in the next section of this text.

3.3. Design of the hybrid ACO & TLBO Model for identification & mitigation of faults

Upon identification of 'non-faulty' nodes, an ACO & TLBO Model is deployed, which assists in value-based checking of nodes for fault evaluation & mitigation during different communications. For each communication, the initially an ACO Model is used to find the shortest path with highest residual energy via the following process,

- Initialize the following ACO parameters,
  - Number of ants (N_a)

International Journal on Recent and Innovation Trends in Computing and Communication
ISSN: 2321-8169 Volume: 10 Issue: 1s
DOI: https://doi.org/10.17762/ijritcc.v10i1s.5821
***Article Received**: 26 August 2022 **Revised**: 31 October 2022 **Accepted**: 23 November 2022*

- Number of iterations (N_i)
- Number of scout ants (N_s)
- Pheromone regulation factor (α)
- Visibility regulation factor (β)
- Pheromone evaporation factor (γ)

- For each iteration in 1 to N_i

- Select N_s number of ants stochastically, and for each ant evaluate node selection probability via equation 10 as follows,

$$p_{ij}^{l} = \frac{\left(\tau_{ij}\right)^{\alpha} * \left(d_{k_{ij}}\right)^{\beta}}{\sum_{h=1}^{N(n)} (\tau_{ih})^{\alpha} * \left(d_{k_{ih}}\right)^{\beta}} \dots (10)$$

Where, $j \in \left(1, N(n)\right)$, while τ represents intensity of pheromone trail between nodes i & j, which is initialized by link quality between the nodes.

- Based on this value of p, evaluate incremental pheromone update via equation 11 as follows,

$$\partial\tau = \frac{Q}{L} \dots (11)$$

Where, L represents maximum distance between the nodes, while Q represents a link quality factor on the path, which is updated by use of network for different communications.

- Using this incremental pheromone update level, reconfigure current number of pheromones on the path via equation 12,

$$p_{ij}^{l}(New) = p_{ij}^{l}(Old) * \gamma + \sum_{h=1}^{N_a} \partial\tau_h \dots (12)$$

- Repeat this process for all iterations, and identify path with maximum pheromones.

Select the identified path, and use for fault-aware routing with high QoS performance. Nodes in the selected path are evaluated via a TLBO model, that assists in identification of fuzzy value changes during communications. This model works via the following process,

- Initialize TLBO Parameters,
- Number of iterations (N_i)
- Number of teachers ($N(T)$)
- Number of learners (N_l)
- Teacher nodes are selected as nodes with higher energy levels in the path, while other nodes are marked as learner nodes.
- For each iteration in 1 to N_i, perform the following tasks,
- Select a stochastic Teacher Node, evaluate its sensor value, and convert this value into fuzzy range of Low (L=1), Medium (M=2), and High (H=3)
- Based on this fuzzy value, identify difference between fuzzy values of any of the stochastic student nodes.
- If difference between the fuzzy values is more than unity, then discard the student node, and increment its faulty count values (FCV).
- At the end of all iterations, identify fault count value threshold via equation 13 as follows,

$$FCV_{th} = \sum_{i=1}^{N_l} FCV_i * \frac{L_r}{N_l} \dots (13)$$

- If any node has $FCV > FCV_{th}$, then mark the node as 'faulty' and shift it to the 'fault node cluster'

Based on this process, faulty nodes are identified, and node clusters are updated. Due to which, the network incrementally shifts nodes from normal clusters to faulty clusters, thereby improving overall network efficiency. This efficiency is further improved via use of incremental learning, for continuous performance improvement. Design of this incremental learning layer is discussed in the next section of this text.

3.4. Design of the incremental learning layer for continuous performance improvement

Based on sections 3.1, 3.2, and 3.3, it can be observed that nodes are intelligently selected for routing & harvesting based on their distance, energy levels, and capacity metrics. This selection is further improved via use of an incremental learning model, that iteratively improves values of L_r for better model performance. To perform this task, a pre-set number of communications are performed, and QoS metrics are measured after each of these communication sets. These metrics include, end to end communication delay, communication energy, throughput, & packet delivery ratio, and are evaluated via equations 14, 15, 16 & 17 respectively,

$$D = \sum_{i=1}^{N_c} \frac{t_{complete_i} - t_{onset_i}}{N_c} \dots (14)$$

Where, $D, t_{complete}$ & t_{onset} represents mean delay for N_c communications, completion timestamp, and onset timestamp for each of the communications.

$$E = \sum_{i=1}^{N_c} \frac{E_{onset_i} - E_{complete_i}}{N_c} \dots (15)$$

Here, E, E_{onset}, & $E_{complete}$ represents mean energy consumption, energy levels during communication onset, and energy levels after completion of the communications.

$$T = \sum_{i=1}^{N_c} \frac{P(RX)}{N_c * D} \dots (16)$$

Where, T & $P(RX)$ represents throughput, and number of packets received successfully during the communications.

International Journal on Recent and Innovation Trends in Computing and Communication
ISSN: 2321-8169 Volume: 10 Issue: 1s
DOI: https://doi.org/10.17762/ijritcc.v10i1s.5821
***Article Received**: 26 August 2022 **Revised**: 31 October 2022 **Accepted**: 23 November 2022*

$$PDR = \sum_{i=1}^{N_c} \frac{P(RX)}{N_c * P(TX)} \dots (17)$$

Where, $PDR, \& P(TX)$ represents packet delivery ratio, and number of packets transmitted during the communications. Based the newer and older values of these QoS metrics, evaluate new value of learning rate via equation 18 as follows,

$$L_r(New) = L_r(Old) * \frac{\left[\frac{D(Old)}{D(New)} + \frac{E(Old)}{E(New)} + \frac{T(New)}{T(Old)} + \frac{PDR(New)}{PDR(Old)}\right]}{4} \dots (18)$$

After updating the value of L_r, if $L_r(New) > L_r(Old)$, that indicates that network's current performance is optimum, and no need of retuning the parameters, otherwise the GA Model is re-evaluated with this new value of L_r and clustering is performed for better performance. Due to these updates, the proposed model is capable of self-tuning its performance for better QoS under different network scenarios. Evaluation of this performance can be observed from the next section of this text.

4. Results analysis & validation

The proposed model uses a combination of different bioinspired optimization techniques to improve clustering, fault tolerance, and energy harvesting performance. To evaluate this performance, the proposed HBMFTEFR model was evaluated under different simulation conditions in terms of end-to-end communication delay, throughput, packet delivery ratio and energy consumption metrics for different communications. These communications were performed under a standard Network configuration scenario, which can be observed from table 1 as follows,

Table 1. Configuration of Network for evaluation under different communication scenarios

Parameter used for Network	**Parameter Value**
Model used for propagation	Two Ray Model with Ground Communications
Used MAC Protocol	802.16a
Interface Queue Used for Evaluation	Priority Queue with Drop Tail for excess packets
Antenna's Model	Omni directional antenna
Number of Nodes in the Network	500 to 2000
Underlying routing protocol	DSR
Dimensions of the Wireless Network	500m x 500 m

Based on these parameters, initially the network model was compared with various energy harvesting models as proposed in IUCP [3], EH IRSP [8], and TEM SEP [16], which will assist readers to identify network's performance w.r.t. state-of-the-art methods. This evaluation can be observed from section 4.1, and was done for 500, 1000, & 2000 nodes under different number of node-to-node communications. Following this, section 4.2 demonstrates performance of the HBMFTEFR model under different types of faults, wherein QoS metrics were compared with NL FFT [25], Co Duch [29], and DPSO [32], which are standard fault tolerance models. Based on this performance readers will be able to identify fault mitigation & tolerance capabilities of the proposed model.

4.1. QoS performance when compared with various state-of-the-art energy harvesting models

Due to inclusion of GA, and ACO, QoS performance of the proposed HBMFTEFR model was observed to be superior when compared with IUCP [3], EH IRSP [8], and TEM SEP [16] deployments. This performance was evaluated by varying number of nodes between 500 to 2000; and estimating the QoS values for different number of communications (NC). The value of NC was varied between 200 to 2000 for simulating small, medium and large sized networks. The final QoS values are estimated by simulating network parameters for each communication, and then averaging them for accurate evaluation of performance. As per this evaluation strategy, values for end-to-end delay (D) for different protocols is tabulated in table 2 as below.

From this evaluation, and figure 3 it can be observed that the proposed model showcases 10.5% lower delay when compared with IUCP [3], 15.2% lower delay when compared with EH IRSP [8], and 18.6% lower delay when compared with TEM SEP [16] due to use of GA & ACO, which assists in estimation of shortest paths. As the number of nodes are increased from 500 to 1000, the delay performance is further optimized.

Table 2. Average communication delay for different energy harvesting models (for 500 Wireless nodes)

No. of Wireless Nodes = 500				
NC	**D (ms) IUCP [3]**	**D (ms) EH IRSP [8]**	**D (ms) TEM SEP [16]**	**D (ms) Proposed**
200	0.94	1.07	1.18	0.67
240	1.04	1.17	1.28	0.72
280	1.13	1.24	1.35	0.76
320	1.16	1.29	1.41	0.79

International Journal on Recent and Innovation Trends in Computing and Communication
ISSN: 2321-8169 Volume: 10 Issue: 1s
DOI: https://doi.org/10.17762/ijritcc.v10i1s.5821
***Article Received**: 26 August 2022 **Revised**: 31 October 2022 **Accepted**: 23 November 2022*

360	1.21	1.36	1.49	0.84
400	1.29	1.45	1.60	0.92
500	1.37	1.63	1.87	1.10
600	1.61	2.12	2.43	1.43
800	2.27	2.77	3.06	1.75
900	2.81	3.16	3.43	1.95
1000	2.98	3.39	3.73	2.14
1100	3.23	3.81	4.21	2.41
1200	3.75	4.35	4.76	2.71
1400	4.22	4.79	5.28	3.02
1600	4.55	5.44	5.98	3.30
2000	4.64	5.64	6.15	3.36

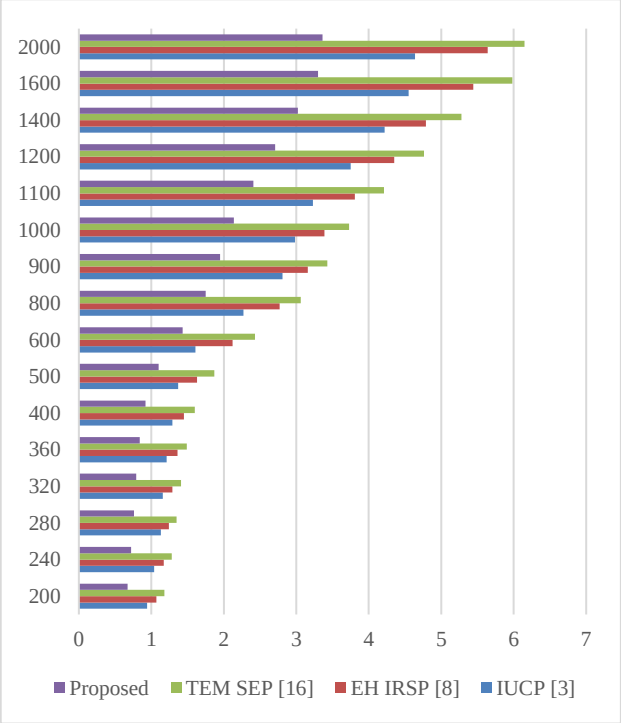

Figure 3. Delay performance of different models

This can be observed from table 3 as follows

Table 3. Average communication delay for different energy harvesting models (for 1000 Wireless nodes)

No. of NC	**D (ms) IUCP [3]**	**D (ms) EH IRSP [8]**	**D (ms) TEM SEP [16]**	**D (ms) Proposed**
200	1.13	1.24	1.47	0.78
240	1.24	1.35	1.59	0.84
280	1.34	1.43	1.67	0.88
320	1.39	1.49	1.75	0.93
360	1.45	1.57	1.85	0.98
400	1.55	1.66	1.99	1.08
500	1.63	1.86	2.33	1.29
600	1.93	2.43	3.05	1.67
800	2.72	3.19	3.83	2.05
900	3.37	3.63	4.29	2.29
1000	3.58	3.89	4.66	2.51
1100	3.87	4.38	5.26	2.83
1200	4.50	5.00	5.95	3.19
1400	5.07	5.50	6.61	3.56
1600	5.46	6.26	7.48	3.88
2000	5.57	6.49	7.69	3.95

From this evaluation it can be observed that the proposed model showcases 14.5% lower delay when compared with IUCP [3], 19.2% lower delay when compared with EH IRSP [8], and 20.3% lower delay when compared with TEM SEP [16] due to use of GA & ACO, which assists in estimation of shortest paths. This delay is further reduced as the number of nodes are increased from 1000 to 2000. This can be observed from table 4 as below.

From this evaluation it can be observed that the proposed model showcases 16.2% lower delay when compared with IUCP [3], 23.1% lower delay when compared with EH IRSP [8], and 24.6% lower delay when compared with TEM SEP [16] due to use of GA & ACO, which assists in estimation of shortest paths.

Table 4. Average communication delay for different energy harvesting models (for 2000 Wireless nodes)

No. of NC	**D (ms) IUCP [3]**	**D (ms) EH IRSP [8]**	**D (ms) TEM SEP [16]**	**D (ms) Proposed**
200	1.37	1.54	1.76	0.90
240	1.51	1.68	1.91	0.97
280	1.64	1.78	2.01	1.02
320	1.69	1.85	2.10	1.07
360	1.78	1.95	2.21	1.14
400	1.89	2.07	2.38	1.24
500	1.99	2.32	2.79	1.48
600	2.35	3.02	3.65	1.93
800	3.32	3.96	4.59	2.37
900	4.11	4.52	5.15	2.64
1000	4.37	4.85	5.59	2.89
1100	4.73	5.45	6.31	3.26
1200	5.49	6.22	7.13	3.68
1400	6.18	6.85	7.93	4.18
1600	6.67	7.79	8.99	4.56

International Journal on Recent and Innovation Trends in Computing and Communication
ISSN: 2321-8169 Volume: 10 Issue: 1s
DOI: https://doi.org/10.17762/ijritcc.v10i1s.5821
***Article Received**: 26 August 2022 **Revised**: 31 October 2022 **Accepted**: 23 November 2022*

2000	6.81	8.07	9.24	4.58

Similar observations are done for energy performance, this can be observed for 500 nodes from table 5 as below.
From this evaluation and figure 4, it can be observed that the proposed model showcases 10.3% lower energy consumption when compared with IUCP [3], 20.5% lower energy consumption when compared with EH IRSP [8], and 18.2% lower energy consumption when compared with TEM SEP [16] due to use of GA & ACO, which assists in estimation of shortest paths with lower residual energy levels.
As the number of nodes are increased from 500 to 1000, the energy performance is further optimized.

Table 5. Average energy consumption for different energy harvesting models (for 500 Wireless nodes)

No. of Wireless Nodes = 500				
NC	**E (mJ) IUCP [3]**	**E (mJ) EH IRSP [8]**	**E (mJ) TEM SEP [16]**	**E (mJ) Proposed**
200	2.16	3.49	3.15	1.84
240	2.65	3.93	3.47	2.01
280	2.77	4.12	3.64	2.12
320	2.91	4.36	3.86	2.25
360	3.09	4.64	4.09	2.37
400	3.29	4.88	4.29	2.48
500	3.42	5.07	4.45	2.58
600	3.56	5.27	4.63	2.68
800	3.70	5.46	4.82	2.80
900	3.82	5.75	5.12	2.98
1000	4.08	6.25	5.52	3.19
1100	4.51	6.60	5.73	3.30
1200	4.57	6.59	5.73	3.27
1400	4.49	6.65	5.39	2.94
1600	4.75	6.99	5.56	3.03
2000	5.02	7.34	6.16	3.46

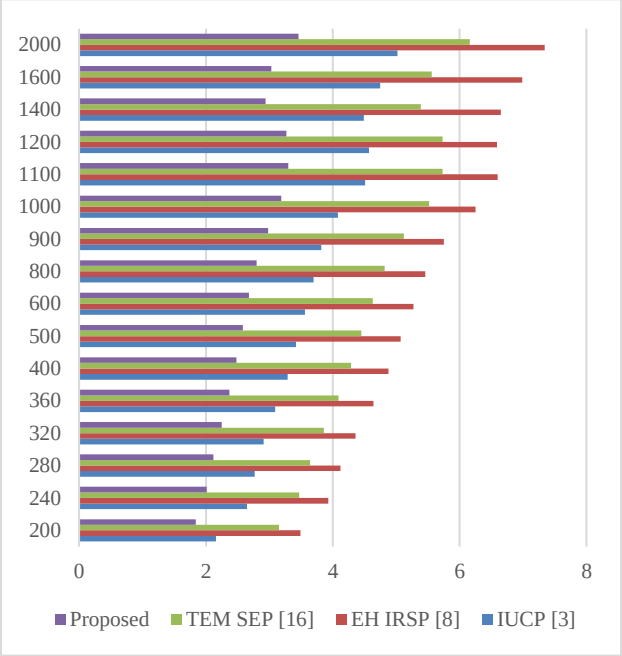

Figure 4. Energy performance of different models

This can be observed from table 6 as follows,

Table 6. Average energy consumption for different energy harvesting models (for 1000 Wireless nodes)

No. of Wireless Nodes = 1000				
NC	**E (mJ) IUCP [3]**	**E (mJ) EH IRSP [8]**	**E (mJ) TEM SEP [16]**	**E (mJ) Proposed**
200	2.59	4.01	3.93	1.98
240	3.18	4.53	4.34	2.17
280	3.31	4.75	4.55	2.28
320	3.49	5.03	4.83	2.41
360	3.72	5.35	5.12	2.55
400	3.95	5.61	5.35	2.67
500	4.10	5.82	5.56	2.78
600	4.27	6.05	5.77	2.88
800	4.43	6.29	6.01	3.02
900	4.59	6.63	6.40	3.22
1000	4.91	7.20	6.90	3.45
1100	5.42	7.60	7.17	3.55
1200	5.49	7.59	7.18	3.52
1400	5.53	7.80	7.42	3.64
1600	5.89	8.23	7.80	3.86
2000	6.11	8.53	8.08	3.99

From this evaluation it can be observed that the proposed model showcases 15.9% lower energy consumption when compared with IUCP [3], 18.3% lower energy consumption when compared with EH IRSP [8], and 20.5% lower energy

International Journal on Recent and Innovation Trends in Computing and Communication
ISSN: 2321-8169 Volume: 10 Issue: 1s
DOI: https://doi.org/10.17762/ijritcc.v10i1s.5821
***Article Received**: 26 August 2022 **Revised**: 31 October 2022 **Accepted**: 23 November 2022*

consumption when compared with TEM SEP [16] due to use of GA & ACO, which assists in estimation of shortest paths with lower residual energy levels. This energy consumption is further reduced as the number of nodes are increased from 1000 to 2000. This can be observed from table 7 as below.

From this evaluation it can be observed that the proposed model showcases 19.5% lower energy consumption when compared with IUCP [3], 23.2% lower energy consumption when compared with EH IRSP [8], and 25.5% lower energy consumption when compared with TEM SEP [16] due to use of GA & ACO, which assists in estimation of shortest paths with lower residual energy levels.

Table 7. Average energy consumption for different energy harvesting models (for 2000 Wireless nodes)

No. of Wireless Nodes = 2000				
NC	**E (mJ) IUCP [3]**	**E (mJ) EH IRSP [8]**	**E (mJ) TEM SEP [16]**	**E (mJ) Proposed**
200	3.17	5.01	4.71	2.18
240	3.89	5.64	5.20	2.38
280	4.06	5.91	5.46	2.51
320	4.27	6.26	5.79	2.66
360	4.54	6.66	6.14	2.82
400	4.83	6.99	6.43	2.94
500	5.02	7.27	6.67	3.06
600	5.21	7.55	6.93	3.18
800	5.42	7.83	7.23	3.33
900	5.61	8.25	7.69	3.55
1000	6.00	8.97	8.29	3.79
1100	6.62	9.47	8.60	3.91
1200	6.70	9.44	8.61	3.88
1400	6.76	9.71	8.90	4.01
1600	7.19	10.25	9.36	4.25
2000	7.47	10.62	9.69	4.40

This assists in deploying the network with better lifetime, and better energy efficiency under different network scenarios. Similar observations are done for throughput performance, this performance is averaged for 500, 1000 and 2000 nodes; and can be observed from table 8 as below.

From this evaluation and figure 6, it can be observed that the proposed model showcases 28.5% higher throughput when compared with IUCP [3], 29.2% higher throughput when compared with EH IRSP [8], and 16.5% higher throughput when compared with TEM SEP [16] due to use of GA & ACO, which assists in estimation of shortest paths with lower residual energy levels & better rate of communication.

Table 8. Average throughput for different energy harvesting models (averaged over 500, 1000 & 2000 Wireless nodes)

Avg. nodes 500 1000 & 2000				
NC	**T (kbps) IUCP [3]**	**T (kbps) EH IRSP [8]**	**T (kbps) TEM SEP [16]**	**T (kbps) Proposed**
200	317.90	332.16	384.17	484.10
240	321.57	334.80	387.00	487.60
280	322.89	336.88	389.67	491.20
320	325.53	339.92	393.17	495.70
360	328.75	343.04	396.67	500.10
400	331.54	345.92	400.09	504.30
500	334.33	348.80	403.51	508.50
600	337.11	351.68	406.84	512.70
800	339.90	354.56	410.17	516.90
900	342.69	357.44	413.51	521.10
1000	345.47	360.32	416.84	525.30
1100	348.26	363.28	420.17	529.50
1200	351.05	366.24	423.51	533.70
1400	353.83	369.12	426.84	537.90
1600	356.62	371.93	430.13	542.04
2000	359.41	374.74	433.41	546.16

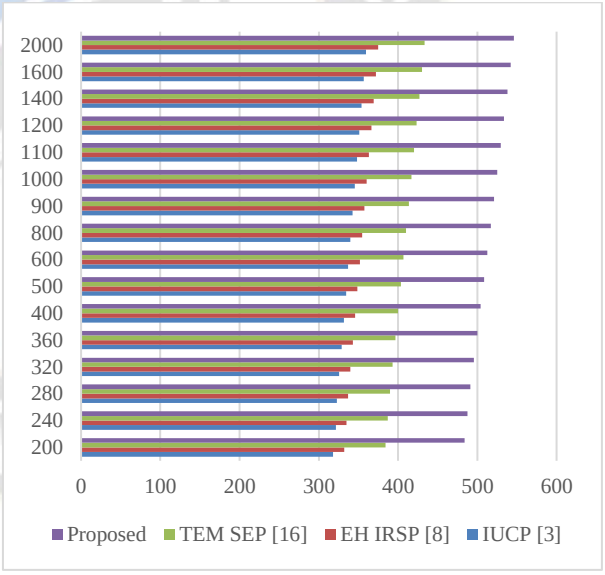

Figure 6. Energy performance of different models

Similar observations are done for packet delivery rate (P) performance, this performance is averaged for 500, 1000 and 2000 nodes. This is done such that the network performance can be evaluated for low, medium and large number of nodes; and can be observed from table 9 as follows,

International Journal on Recent and Innovation Trends in Computing and Communication
ISSN: 2321-8169 Volume: 10 Issue: 1s
DOI: https://doi.org/10.17762/ijritcc.v10i1s.5821
***Article Received**: 26 August 2022 **Revised**: 31 October 2022 **Accepted**: 23 November 2022*

Table 9. Average packet delivery ratio performance for different energy harvesting models (averaged over 500, 1000 & 2000 Wireless nodes)

Avg. nodes	500	1000 &	2000
NC	PDR(%) IUCP [3]	PDR (%) EH IRSP [8]	PDR (%) TEM SEP [16]	PDR (%) Proposed
200	82.78	82.53	83.46	88.05
240	83.74	83.17	84.08	88.70
280	84.09	83.69	84.65	89.34
320	84.78	84.45	85.43	90.15
360	85.62	85.23	86.19	90.95
400	86.34	85.94	86.92	91.72
500	87.06	86.66	87.64	92.48
600	87.79	87.38	88.37	93.24
800	88.52	88.10	89.10	94.01
900	89.24	88.82	89.82	94.78
1000	89.96	89.54	90.55	95.54
1100	90.69	90.26	91.28	96.30
1200	91.42	90.97	92.00	97.07
1400	92.14	91.70	92.72	97.84
1600	92.87	92.42	93.45	98.61
2000	93.60	93.12	94.16	99.36

From this evaluation and figure 7, it can be observed that the proposed model showcases 5.5% higher PDR when compared with IUCP [3], 6.1% higher PDR when compared with EH IRSP [8], and 3.8% higher PDR when compared with TEM SEP [16] due to use of GA & ACO, which assists in estimation of shortest paths with lower residual energy levels & better rate of communication. These evaluations are extended for different number of faults in the network, and can be observed from the next section.

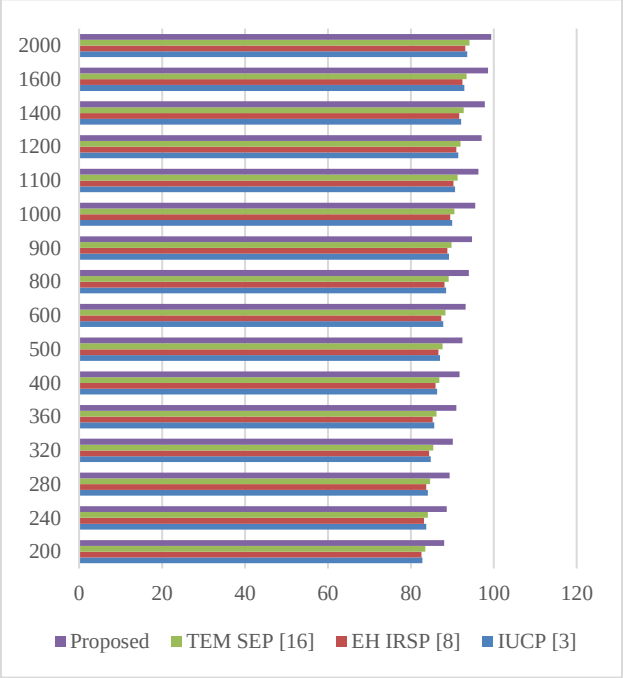

Figure 7. Throughput performance of different models

4.3. Fault tolerance performance of different communication models in presence different faults

Due to inclusion of fault tolerance during trust-enabled routing via use of PSO & TLBO, the QoS performance of the proposed HBMFTEFR model is superior when compared with NL FFT [25], Co Duch [29], and DPSO [32] models under different fault types. This performance is estimated by varying number of faulty nodes (NF) nodes between 2% to 40%; and estimating the QoS values. The average QoS values are estimated by simulating the network for 500 communications, and then averaging them for each of these simulations. Due to this, performance comparison, readers can identify characteristics of the proposed model under different fault conditions. As per this evaluation strategy, values for end-to-end delay (D) for different protocols is tabulated in table 10 as follows,

Table 10. Average end-to-end delay for different models (under fault)

NF (%)	D (ms) NL FFT [25]	D (ms) Co Duch [29]	D (ms) DPSO [32]	D (ms) Proposed
2	0.58	0.56	0.62	0.41
4	0.63	0.61	0.66	0.44
6	0.67	0.64	0.69	0.47
10	0.69	0.67	0.73	0.49
16	0.73	0.71	0.79	0.51
20	0.78	0.78	0.89	0.57

International Journal on Recent and Innovation Trends in Computing and Communication
ISSN: 2321-8169 Volume: 10 Issue: 1s
DOI: https://doi.org/10.17762/ijritcc.v10i1s.5821
***Article Received**: 26 August 2022 **Revised**: 31 October 2022 **Accepted**: 23 November 2022*

22	0.89	0.95	1.10	0.68
24	1.13	1.23	1.38	0.87
26	1.47	1.49	1.65	1.07
28	1.70	1.66	1.83	1.20
30	1.83	1.82	2.02	1.31
32	2.05	2.05	2.27	1.47
34	2.33	2.31	2.55	1.66
36	2.59	2.57	2.90	1.86
38	2.88	3.10	3.52	2.19
40	2.95	3.23	3.63	2.26

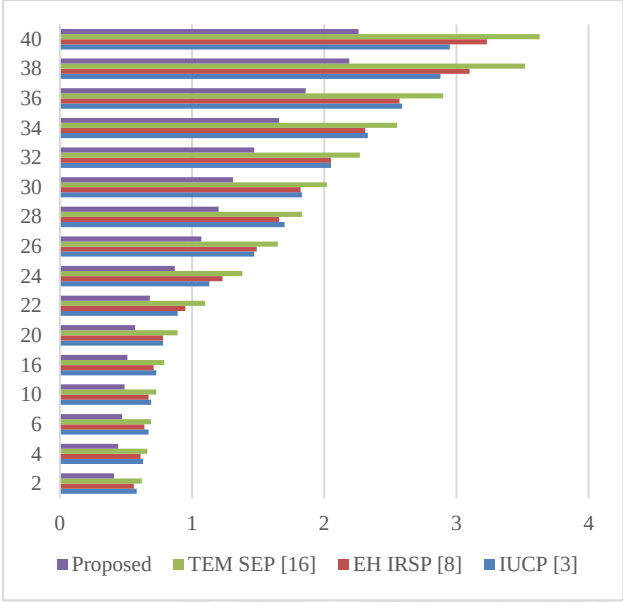

Figure 8. Delay performance under faults

From this evaluation and figure 8, it can be observed that the proposed model showcases 9.2% lower delay when compared with NL FFT [25], 14.5% lower delay when compared with Co Duch [29], and 16.8% lower delay when compared with DPSO [32] due to use of GA & ACO with PSO & TLBO, which assists in estimation of shortest paths even under faults. Similar observations are done for energy performance, and can be observed from table 11 as follows,

Table 11. Average energy consumption for different models (under faults)

NF (%)	**E (mJ) NL FFT [25]**	**E (mJ) Co Duch [29]**	**E (mJ) DPSO [32]**	**E (mJ) Proposed**
2	1.27	1.12	1.32	0.82
4	1.44	1.22	1.42	0.91
6	1.51	1.28	1.50	0.96
10	1.61	1.36	1.59	1.01
16	1.70	1.44	1.68	1.07
20	1.79	1.50	1.75	1.12
22	1.86	1.56	1.81	1.17
24	1.93	1.63	1.89	1.21
26	2.01	1.71	1.99	1.27
28	2.12	1.82	2.13	1.35
30	2.28	1.93	2.27	1.44
32	2.41	2.06	2.42	1.53
34	2.58	2.23	2.62	1.65
36	2.82	2.43	2.88	1.80
38	3.07	2.71	3.22	2.00
40	3.14	2.76	3.27	2.04

From this evaluation and figure 9, it can be observed that the proposed model showcases 20.3% lower energy consumption when compared with NL FFT [25], 24.8% lower energy consumption when compared with Co Duch [29], and 15.3% lower energy consumption when compared with DPSO [32] due to use of GA & ACO with PSO & TLBO, which assists in estimation of shortest paths with better energy efficiency even under faults.

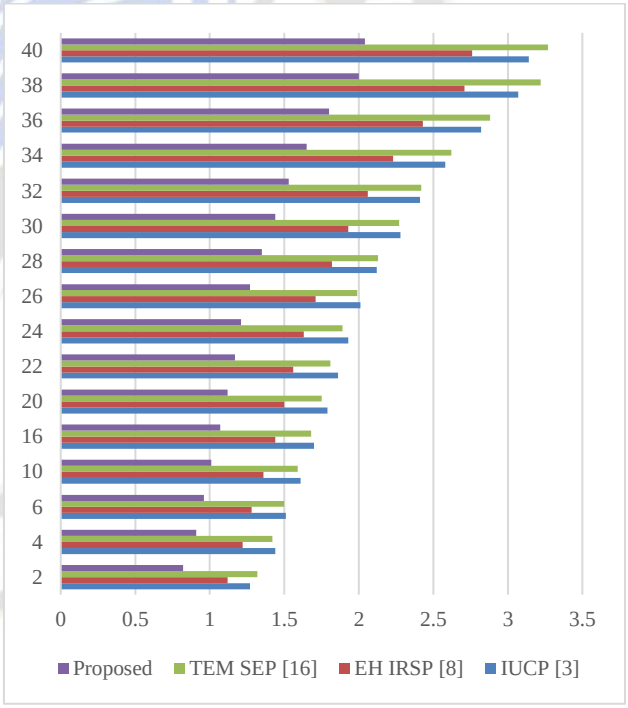

Figure 9. Energy consumption of different models under fault conditions

Similar observations are done for throughput performance and can be observed from table 12 as follows,

International Journal on Recent and Innovation Trends in Computing and Communication
ISSN: 2321-8169 Volume: 10 Issue: 1s
DOI: https://doi.org/10.17762/ijritcc.v10i1s.5821
***Article Received**: 26 August 2022 **Revised**: 31 October 2022 **Accepted**: 23 November 2022*

Table 12. Average throughput performance for different models (under faults)

NF (%)	T (kbps) NL FFT [25]	T (kbps) Co Duch [29]	T (kbps) DPSO [32]	T (kbps) Proposed
2	194.19	251.48	232.58	277.20
4	195.85	253.34	234.29	279.28
6	197.07	255.20	236.15	281.32
10	198.77	257.51	238.27	283.87
16	200.62	259.83	240.38	286.42
20	202.33	261.99	242.44	288.82
22	204.04	264.15	244.45	291.22
24	205.74	266.36	246.46	293.61
26	207.39	268.52	248.47	296.01
28	209.10	270.68	250.48	298.41
30	210.81	272.89	252.49	300.81
32	212.46	275.10	254.50	303.20
34	214.17	277.26	255.66	305.28
36	215.87	276.06	245.00	301.22
38	212.36	237.56	184.19	259.54
40	212.74	232.15	179.92	255.76

From this evaluation and figure 10 it can be observed that the proposed model showcases 16.2% higher throughput when compared with NL FFT [25], 9.4% higher throughput when compared with Co Duch [29], and 28.5% higher throughput when compared with DPSO [32] due to use of GA & ACO with PSO & TLBO, which assists in estimation of shortest paths with better energy efficiency & higher packet rates even under faults.

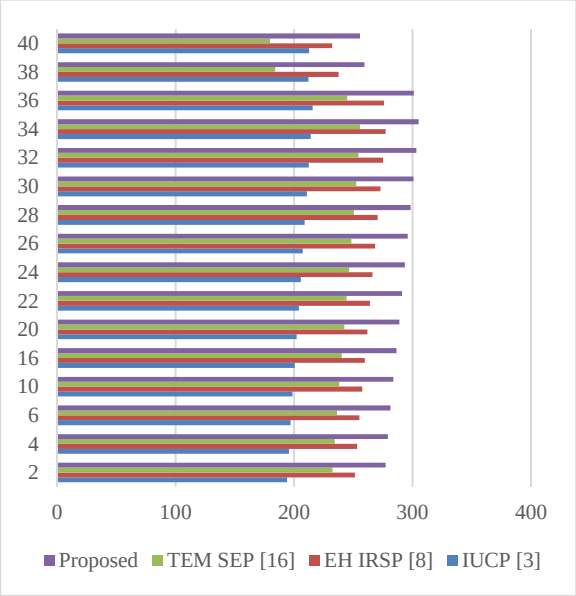

Figure 10. Average throughput performance for different models (under faults)

Similar observations are done for packet delivery rate (P) performance, and can be observed from table 13 as below.

From this evaluation and figure 11, it can be observed that the proposed model showcases 18.5% higher PDR when compared with NL FFT [25], 26.1% higher PDR when compared with Co Duch [29], and 19.2% higher PDR when compared with DPSO [32] due to use of GA & ACO with PSO & TLBO, which assists in estimation of shortest paths with better energy efficiency & higher packet rates even under faults.

Table 13. Average Packet Delivery Ratio performance for different models (under faults)

NA (%)	PDR(%) NL FFT [25]	PDR(%) Co Duch [29]	PDR(%) DPSO [32]	PDR (%) Proposed
2	70.37	63.86	68.88	87.17
4	71.18	64.36	69.39	87.81
6	71.47	64.75	69.86	88.45
10	72.06	65.33	70.49	89.25
16	72.77	65.93	71.13	90.04
20	73.39	66.49	71.73	90.80
22	74.01	67.05	72.33	91.56
24	74.63	67.61	72.92	92.32
26	75.24	68.16	73.52	93.07
28	75.86	68.72	74.13	93.83
30	76.47	69.28	74.73	94.59
32	77.09	69.84	75.33	95.35
34	77.71	70.39	75.93	96.10
36	78.33	70.94	76.52	96.86
38	78.94	71.50	77.12	97.63
40	79.55	72.04	77.71	98.37

International Journal on Recent and Innovation Trends in Computing and Communication
ISSN: 2321-8169 Volume: 10 Issue: 1s
DOI: https://doi.org/10.17762/ijritcc.v10i1s.5821
***Article Received**: 26 August 2022 **Revised**: 31 October 2022 **Accepted**: 23 November 2022*

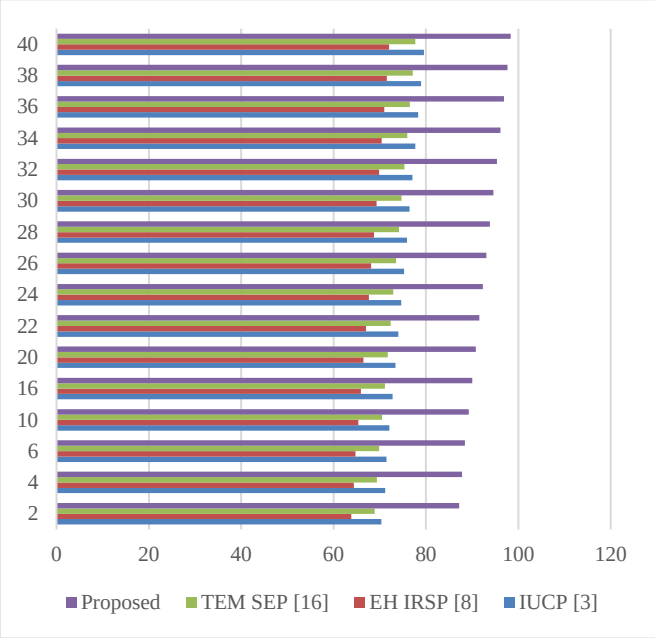

Figure 11. Average Packet Delivery Ratio performance for different models (under faults)

Based on this performance evaluation, it can be observed that the proposed model has higher fault tolerance, and showcases better path evaluations under different network conditions, thereby making it useful for a wide variety of real-time network deployments.

5. Conclusion and future work

The proposed model uses a combination of different bioinspired models for optimization of different network parameters. Here, GA is used for initial clustering, which assists in identification of energy harvesting nodes, this is supported by PSO model, that evaluates faulty nodes, and uses them as backup for continuous energy harvesting process. These models are further extended via use of an ACO based TLBO Model that incorporates fuzzy rule-based value checks, along with delay-aware, energy-aware can capacity-aware nodes for routing in dense wireless network environments. Performance of the proposed model was evaluated w.r.t. various energy efficient & fault tolerant models, and it was observed that the proposed model showcased 14.5% lower delay when compared with IUCP [3], 19.2% lower delay when compared with EH IRSP [8], and 20.3% lower delay when compared with TEM SEP [16] due to use of GA & ACO, which assists in estimation of shortest paths. Similarly, it showcased 10.3% lower energy consumption when compared with IUCP [3], 20.5% lower energy consumption when compared with EH IRSP [8], and 18.2% lower energy consumption when compared with TEM SEP [16] due to use of GA & ACO, which assists in estimation of shortest paths with lower residual energy levels. The model also showcased 28.5% higher throughput when compared with IUCP [3], 29.2% higher throughput when compared with EH IRSP [8], and 16.5% higher throughput when compared with TEM SEP [16] due to use of GA & ACO, which assists in estimation of shortest paths with lower residual energy levels & better rate of communications. Under faulty conditions, the proposed model showcases 9.2% lower delay when compared with NL FFT [25], 14.5% lower delay when compared with Co Duch [29], and 16.8% lower delay when compared with DPSO [32] due to use of GA & ACO with PSO & TLBO, which assists in estimation of shortest paths even under faults. Similarly, the proposed model showcased 16.2% higher throughput when compared with NL FFT [25], 9.4% higher throughput when compared with Co Duch [29], and 28.5% higher throughput when compared with DPSO [32] due to use of GA & ACO with PSO & TLBO, which assists in estimation of shortest paths with better energy efficiency & higher packet rates even under faults. Due to which, it is capable of high efficiency energy harvesting, and fault tolerant applications. In future, the proposed model must be evaluated under different types of network scenarios, and must be integrated with Deep Learning, Q-Leaning, and Reinforcement learning to further optimize its real time performance. Moreover, blockchain technologies can be integrated to the model to further strengthen its security under real-time deployment scenarios.

References

[1]. Y. Luo and L. Pu, "Practical Issues of RF Energy Harvest and Data Transmission in Renewable Radio Energy Powered IoT," in IEEE Transactions on Sustainable Computing, vol. 6, no. 4, pp. 667-678, 1 Oct.-Dec. 2021, doi: 10.1109/TSUSC.2020.3000085.

[2]. Y. Wang, K. Yang, W. Wan, Y. Zhang and Q. Liu, "Energy-Efficient Data and Energy Integrated Management Strategy for IoT Devices Based on RF Energy Harvesting," in IEEE Internet of Things Journal, vol. 8, no. 17, pp. 13640-13651, 1 Sept.1, 2021, doi: 10.1109/JIOT.2021.3068040.

[3]. Q. Ren and G. Yao, "Enhancing Harvested Energy Utilization for Energy Harvesting Wireless Sensor Networks by an Improved Uneven Clustering Protocol," in IEEE Access, vol. 9, pp. 119279-119288, 2021, doi: 10.1109/ACCESS.2021.3108469.

[4]. K. Moon, K. M. Kim, Y. Kim and T. -J. Lee, "Device-Selective Energy Request in RF Energy-Harvesting Networks," in IEEE Communications Letters, vol. 25, no. 5, pp. 1716-1719, May 2021, doi: 10.1109/LCOMM.2021.3053761.

[5]. D. Ghosh, M. K. Hanawal and N. Zlatanov, "Learning to Optimize Energy Efficiency in Energy Harvesting Wireless

Sensor Networks," in IEEE Wireless Communications Letters, vol. 10, no. 6, pp. 1153-1157, June 2021, doi: 10.1109/LWC.2021.3058170.

[6]. Z. J. Chew, T. Ruan and M. Zhu, "Energy Savvy Network Joining Strategies for Energy Harvesting Powered TSCH Nodes," in IEEE Transactions on Industrial Informatics, vol. 17, no. 2, pp. 1505-1514, Feb. 2021, doi: 10.1109/TII.2020.3005196.

[7]. Y. Sun, C. Song, S. Yu, Y. Liu, H. Pan and P. Zeng, "Energy-Efficient Task Offloading Based on Differential Evolution in Edge Computing System With Energy Harvesting," in IEEE Access, vol. 9, pp. 16383-16391, 2021, doi: 10.1109/ACCESS.2021.3052901.

[8]. A. Khan et al., "EH-IRSP: Energy Harvesting Based Intelligent Relay Selection Protocol," in IEEE Access, vol. 9, pp. 64189-64199, 2021, doi: 10.1109/ACCESS.2020.3044700.

[9]. J. Huang, B. Yu, C. -C. Xing, T. Cerny and Z. Ning, "Online Energy Scheduling Policies in Energy Harvesting Enabled D2D Communications," in IEEE Transactions on Industrial Informatics, vol. 17, no. 8, pp. 5678-5687, Aug. 2021, doi: 10.1109/TII.2020.3005440.

[10]. A. Jaitawat and A. K. Singh, "Online Transmission Policy for Energy Harvesting Sensor Node With Energy Loss," in IEEE Communications Letters, vol. 25, no. 2, pp. 551-554, Feb. 2021, doi: 10.1109/LCOMM.2020.3028767.

[11]. Y. Cheng, W. Xia, H. Zhao, L. Yang and H. Zhu, "Joint Caching and User Association for Energy Harvesting Aided Internet of Things with Full-Duplex Backhauls," in Journal of Communications and Information Networks, vol. 6, no. 4, pp. 420-428, Dec. 2021, doi: 10.23919/JCIN.2021.9663106.

[12]. E. Cui, D. Yang, H. Zhang and M. Gidlund, "Improving Power Stability of Energy Harvesting Devices With Edge Computing-Assisted Time Fair Energy Allocation," in IEEE Transactions on Green Communications and Networking, vol. 5, no. 1, pp. 540-551, March 2021, doi: 10.1109/TGCN.2020.3046319.

[13]. A. Hoseinghorban, M. R. Bahrami, A. Ejlali and M. A. Abam, "CHANCE: Capacitor Charging Management Scheme in Energy Harvesting Systems," in IEEE Transactions on Computer-Aided Design of Integrated Circuits and Systems, vol. 40, no. 3, pp. 419-429, March 2021, doi: 10.1109/TCAD.2020.3003295.

[14]. J. -S. Lee and H. -T. Jiang, "An Extended Hierarchical Clustering Approach to Energy-Harvesting Mobile Wireless Sensor Networks," in IEEE Internet of Things Journal, vol. 8, no. 9, pp. 7105-7114, 1 May1, 2021, doi: 10.1109/JIOT.2020.3038215.

[15]. A. S. H. Abdul-Qawy, A. B. Nasser, A. H. Guroob, A. -M. H. Y. Saad, N. A. M. Alduais and N. Khatri, "TEMSEP: Threshold-Oriented and Energy-Harvesting Enabled Multilevel SEP Protocol for Improving Energy-Efficiency of Heterogeneous WSNs," in IEEE Access, vol. 9, pp. 154975-155002, 2021, doi: 10.1109/ACCESS.2021.3128507.

[16]. D. A. Temesgene, M. Miozzo, D. Gündüz and P. Dini, "Distributed Deep Reinforcement Learning for Functional Split Control in Energy Harvesting Virtualized Small Cells," in IEEE Transactions on Sustainable Computing, vol. 6, no. 4, pp. 626-640, 1 Oct.-Dec. 2021, doi: 10.1109/TSUSC.2020.3025139.

[17]. E. Stai and V. Karyotis, "Optimal Resource Allocation in Multihop Wireless Networks Relying on Energy Harvesting," in IEEE Communications Letters, vol. 25, no. 1, pp. 224-228, Jan. 2021, doi: 10.1109/LCOMM.2020.3023173.

[18]. K. Ali and D. J. Rogers, "An Orientation-Independent Multi-Input Energy Harvesting Wireless Sensor Node," in IEEE Transactions on Industrial Electronics, vol. 68, no. 2, pp. 1665-1674, Feb. 2021, doi: 10.1109/TIE.2020.2967719.

[19]. T. Wang, S. Wu, Z. Wang, Y. Jiang, T. Ma and Z. Yang, "A Multi-Featured Actor-Critic Relay Selection Scheme for Large-Scale Energy Harvesting WSNs," in IEEE Wireless Communications Letters, vol. 10, no. 1, pp. 180-184, Jan. 2021, doi: 10.1109/LWC.2020.3030695.

[20]. Dash, D. Plane sweep algorithms for data collection for energy harvesting wireless sensor networks using mobile sink. J Ambient Intell Human Comput (2022). https://doi.org/10.1007/s12652-022-03803-2

[21]. Al-Qamaji, A., Atakan, B. Event Distortion-Based Clustering Algorithm for Energy Harvesting Wireless Sensor Networks. Wireless Pers Commun 123, 3823–3843 (2022). https://doi.org/10.1007/s11277-021-09316-z

[22]. M. P. Michaelides and C. G. Panayiotou, "Fault Tolerant Maximum Likelihood Event Localization in Sensor Networks Using Binary Data," in IEEE Signal Processing Letters, vol. 16, no. 5, pp. 406-409, May 2009, doi: 10.1109/LSP.2009.2016481.

[23]. M. Z. A. Bhuiyan, G. Wang, J. Cao and J. Wu, "Deploying Wireless Sensor Networks with Fault-Tolerance for Structural Health Monitoring," in IEEE Transactions on Computers, vol. 64, no. 2, pp. 382-395, Feb. 2015, doi: 10.1109/TC.2013.195.

[24]. S. Hu and G. Li, "Fault-Tolerant Clustering Topology Evolution Mechanism of Wireless Sensor Networks," in IEEE Access, vol. 6, pp. 28085-28096, 2018, doi: 10.1109/ACCESS.2018.2841963.

[25]. V. K. Menaria, S. C. Jain, N. Raju, R. Kumari, A. Nayyar and E. Hosain, "NLFFT: A Novel Fault Tolerance Model Using Artificial Intelligence to Improve Performance in Wireless Sensor Networks," in IEEE Access, vol. 8, pp. 149231-149254, 2020, doi: 10.1109/ACCESS.2020.3015985.

[26]. Y. Tong, L. Tian, L. Lin and Z. Wang, "Fault Tolerance Mechanism Combining Static Backup and Dynamic Timing Monitoring for Cluster Heads," in IEEE Access,

vol. 8, pp. 43277-43288, 2020, doi: 10.1109/ACCESS.2020.2977759.

[27]. H. Shen and Z. Li, "A Kautz-Based Wireless Sensor and Actuator Network for Real-Time, Fault-Tolerant and Energy-Efficient Transmission," in IEEE Transactions on Mobile Computing, vol. 15, no. 1, pp. 1-16, 1 Jan. 2016, doi: 10.1109/TMC.2015.2407391.

[28]. I. -R. Chen, A. P. Speer and M. Eltoweissy, "Adaptive Fault-Tolerant QoS Control Algorithms for Maximizing System Lifetime of Query-Based Wireless Sensor Networks," in IEEE Transactions on Dependable and Secure Computing, vol. 8, no. 2, pp. 161-176, March-April 2011, doi: 10.1109/TDSC.2009.54.

[29]. G. Huang, Y. Zhang, J. He and J. Cao, "Fault Tolerance in Data Gathering Wireless Sensor Networks," in The Computer Journal, vol. 54, no. 6, pp. 976-987, June 2011, doi: 10.1093/comjnl/bxr027.

[30]. Y. Ouyang, Q. Wang, M. Ru, H. Liang and J. Li, "A Novel Low-Latency Regional Fault-Aware Fault-Tolerant Routing Algorithm for Wireless NoC," in IEEE Access, vol. 8, pp. 22650-22663, 2020, doi: 10.1109/ACCESS.2020.2970215.

[31]. Tsang-Yi Wang, Y. S. Han and P. K. Varshney, "Fault-tolerant distributed classification based on non-binary codes in wireless sensor networks," in IEEE Communications Letters, vol. 9, no. 9, pp. 808-810, Sept. 2005, doi: 10.1109/LCOMM.2005.1506710.

[32]. W. Guo, J. Li, G. Chen, Y. Niu and C. Chen, "A PSO-Optimized Real-Time Fault-Tolerant Task Allocation Algorithm in Wireless Sensor Networks," in IEEE Transactions on Parallel and Distributed Systems, vol. 26, no. 12, pp. 3236-3249, 1 Dec. 2015, doi: 10.1109/TPDS.2014.2386343.

[33]. T. Wang, L. Chang, D. Duh and J. Wu, "Fault-tolerant decision fusion via collaborative sensor fault detection in wireless sensor networks," in IEEE Transactions on Wireless Communications, vol. 7, no. 2, pp. 756-768, February 2008, doi: 10.1109/TWC.2008.060653.

[34]. G. Mehmood, M. Z. Khan, S. Abbas, M. Faisal and H. U. Rahman, "An Energy-Efficient and Cooperative Fault-Tolerant Communication Approach for Wireless Body Area Network," in IEEE Access, vol. 8, pp. 69134-69147, 2020, doi: 10.1109/ACCESS.2020.2986268.